Thermal Detection of Cardiac Biomarkers H-FABP and ST2 Using a Molecularly Imprinted Nanoparticle-Based Multiplex Sensor Platform

Robert D. Crapnell[a], Francesco Canfarotta[b*], Joanna Czulak[b], Rhiannon Johnson[b], Kai Betlem[a], Francesco Mecozzi[a], Michael P. Down[a], Kasper Eersels[c], Bart van Grinsven[c], Thomas J. Cleij[c], Richard Law[d], Craig E. Banks[a], Marloes Peeters[d*]

A) Manchester Metropolitan University, Department of Natural Sciences, John Dalton Building, Chester Street, M1 5GD, Manchester, United Kingdom.

B) MIP Diagnostics Ltd., The Exchange Building, Colworth Park, Sharnbrook, MK44 1LQ, Bedford, United Kingdom.

C) Sensor Engineering, Faculty of Science and Engineering, Maastricht University, P.O. Box 616, 6200 MD Maastricht, The Netherlands.

D) Newcastle University, School of Engineering, Merz Court, NE1 7RU, Newcastle Upon Tyne, United Kingdom.

KEYWORDS: Biosensors, Thermal Detection, Heat-Transfer Method, Cardiac Biomarkers, ST2, Heart-Fatty Acid Binding Protein (H-FABP), Molecularly Imprinted Polymer nanoparticles (nanoMIPs).

ABSTRACT: This manuscript describes the production of Molecularly Imprinted Polymer nanoparticles (nanoMIPs) for the cardiac biomarkers heart-fatty acid binding protein (H-FABP) and ST2 by solid-phase synthesis, and their use as synthetic antibodies in a multiplexed sensing platform. Analysis by Surface Plasmon Resonance (SPR) shows that the affinity of the nanoMIPs is similar to that of commercially available antibodies. The particles are coated onto the surface of thermocouples and inserted into 3D-printed flow cells of different multiplexed designs. We demonstrate it is possible to selectively detect both cardiac biomarkers within the physiologically relevant range. Furthermore, the developed sensor platform is the first example of a multiplex format of this thermal analysis technique which enables simultaneous measurements of two different compounds with minimal cross selectivity. The format where three thermocouples are positioned in parallel exhibits the highest sensitivity, which is explained by modelling the heat flow distribution within the flow cell. This design is used in further experiments and proof-of-application of the sensor platform is provided by measuring spiked fetal bovine serum samples. Due to the high selectivity, short measurement time, and low-cost of this array format, it provides an interesting alternative to traditional immunoassays. The use of nanoMIPs enables a multi-marker strategy, which has the potential to contribute to sustainable healthcare by improving reliability of cardiac biomarker testing.

The onset of acute chest pain is one of the most common reasons for emergency department attendance.[1] Diagnostic cornerstones for patients exhibiting these symptoms include clinical assessment, performing an electrocardiogram (ECG), and measurements of cardiac biomarker levels.[2] Early diagnosis of acute coronary syndrome (ACS), for which chest pain is one of the main symptoms, significantly impacts patient morbidity and mortality.[3] Out of the patients with acute chest pain, an estimate of merely 20 % are suffering from ACS. Due to difficulty in the reliable identification of these patients, hospital admission with biomarker measurements has been the standard protocol.[4] In 2016, the European Society of Cardiology recommended 1-hour and 3-hour rule-out strategies for Acute Myocardial Infarction (AMI), which involved the use of highly sensitive cardiac troponin (hs-cTn) assays.[5] Strategies that consider these assays include the Manchester ACS (MACS)[6] and Troponin-only (T-MACS)[7], which have been able to highly accurately (sensitivity 99.1 %) determine the probability that a patient will undergo a major adverse cardiac event within 30 days.[8] The MACS rule incorporates high sensitivity troponin T (hs-TnT), heart fatty acid binding protein (H-FABP), ECG findings and clinical data; whereas T-MACS excludes H-FABP as a variable. Reliability of these rule-out strategies can be enhanced if, besides troponin, other biomarkers are considered, which could include H-FABP (as shown in MACS) and ST2. The first is a cytoplasmic protein of molecular weight 15 kDa with serum levels in healthy humans ranging between 0 – 2.8 ng/mL.[9] Upon experiencing an ischemic episode, H-FABP is quickly released from the myocardial cells, whereas troponin levels gradually increase over the course of a few hours.[10] Hoffman *et al.*, reported that additional H-FABP measurements improve the diagnostic specificity of a NT-proBNP assay to rule out acute heart failure.[11] McCann *et al.*, demonstrated that determination of H-FABP and troponin-T levels offer the best diagnostic sensitivity over all timepoints.[12] Soluble ST2 is a member of the interleukin receptor family and increases in serum levels have been reported to be proportional to the severity of heart failure.[13] The Framingham Heart Study showed that the soluble ST2 levels in plasma varied

from 9 – 45 ng/mL, with significant differences reported depending on age and gender.[14] As increases in ST2 are not universal, they are less suitable as a prognostic marker, but can still offer valuable information when used in combination with other biomarkers.[15] Ho *et al.*, have suggested that soluble ST2 has a role in the prediction of cardiovascular outcome when a multi-marker strategy, including troponin and BNP, is considered.[16] Therefore, there is high demand to develop assays for the simultaneous measurement of multiple cardiac biomarkers in a fast, simple and low-cost manner to enhance the reliability of patient diagnosis. In this manuscript, we focus on H-FABP and ST2 and discuss a sensor platform for the simultaneous determination of these cardiac biomarkers by combining Molecularly Imprinted Polymers (MIPs) as recognition elements alongside thermal detection. MIPs are formed *via* a process in which monomers and cross-linker self-assemble around the target molecule, according to the exposed functionalities. The resulting polymerization process 'freezes' the monomers in place and effectively creates specific binding sites. Removal of the target molecule empties these binding sites, which are then able to re-bind the target molecule.[17,18] High affinity MIP nanoparticles (nanoMIPs) can be produced through a solid-phase approach, which involves polymerization around the template that is covalently attached to a solid support.[19] These nanoMIPs exhibit good biocompatibility[20] and possess superior thermal and chemical stability compared to their natural counterparts, while maintaining high affinity[21].

In previous research, we have demonstrated that nanoMIPs can be dip-coated onto thermocouples and used to detect biomolecules in buffered solutions by monitoring the temperature of a liquid in a flow cell.[22] This strategy is limited to monitoring of a single compound and has not been applied to clinical samples due to issues with matrix effects. Herein, we will describe the development of two novel high affinity nanoMIPs for H-FABP and ST2 that have not been reported in literature and demonstrate that we can measure these molecules at physiologically relevant concentrations using thermal analysis. A novel flow cell design will be presented that enables array formatting, an internal control and has the potential for simultaneous biomarker measurements. This new thermal sensor platform holds great promise for therapeutic and diagnostics due to its simplicity, low-cost, and high sensitivity and selectivity of the nanoMIPs.

Experimental Section: Chemicals Phosphate buffered saline (PBS) solutions were made using PBS tablets (Sigma, UK) and de-ionized water of resistivity not less than 18.2 MΩ cm. Fetal bovine serum (FBS) was purchased from Sigma (UK) and used without any modification. Heart fatty acid binding protein (H-FABP) was purchased from ATGen (US) and ST2 was purchased from Abcam (Cambridge, UK). Chemicals and equipment for the synthesis and analysis of the nanoMIPs are presented in Canfarotta *et al.*[20a]

Synthesis of H-FABP and ST2 nanoMIPs Protocol was adapted from Canfarotta *et al*.[20a] Briefly, glass beads (diameter between 70 – 100 µm) were activated with 2 M NaOH and subsequently functionalized with a silane group to obtain beads with free amine groups on the surface. The target proteins were immobilized onto the amine-derivatized glass beads *via* glutaraldehyde coupling. Immobilization of H-FABP and ST2 was confirmed by monitoring colour changes with bicinchonic acid assay. NanoMIPs were prepared according to a proprietary modified version of the protocol described in Canfarotta *et al.*[20a], which involves radical polymerization of functional and crosslinker monomers at room temperature for 2 h. After polymerization, the solid support was used to isolate the high-affinity nanoMIPs from the remaining monomers, oligomers and low-affinity polymers. This was achieved by first using a low temperature elution followed by an elevated temperature elution (~60 °C).[19]

Size and Concentration Analysis of nanoMIPs The particle size was measured with a Zetasizer Nano (Nano-S) particle-size analyzer (Malvern Instruments Ltd., UK) at 25 °C. Biacore analysis was performed on SIA Au SPR gold chips (GE Healthcare) that were modified with mercaptoundecaonic acid onto which nanoMIPs were coupled *via* EDC/NHS chemistry. Flow conditions were set at 30 µL/min and excess NHS esters were deactivated by injecting with 100 µL of ethanolamine hydrochloride (0.1 M) at 10 µL/min. Five different concentrations of the target protein (0.05 – 250 nM) in PBS were injected. A control channel functionalized with nanoMIPs produced for target trypsin using the same monomer and cross-linker composition was used as a negative control. The dissociation time was set at 5 min and the data was analyzed using BiaEvaluation software (v 4.1) to obtain K_d values.

Thermal Measurements of nanoMIPs Sensors The MIP-functionalized thermocouples were prepared according to the protocol from Canfarotta *et al*. as seen in the Supporting Information (Figure S-1).[22] Type K thermocouples (RS Components, UK) were exposed to solutions of nanoMIPs in water for 1 min, with an insertion and withdrawing rate of 5.1 cm/min. After drying (2 h), the functionalized thermocouples were inserted into flows cells fabricated in-house through 3D printing (Supporting Information S-2). These were produced on a FORM 2 stereolithography 3D-Printer (FormLabs, USA) using FORM 2 Clear Resin (GPCL04). The flow cells were subsequently coupled to a heat-transfer device as described by van Grinsven *et al*.[23] The device was steered with LabView software that actively controls the temperature of the copper block (T_1). A proportional-integral-derivative (PID) controller that is attached a power resistor (22 Ω) regulated the feedback on the signal.[24] In this work, the PID parameters were optimized through tuning experiments. These values were defined as 1: 14: 0.3 and these were used throughout the experiments. In all sensing measurements presented within this manuscript, the temperature was kept constant at 37.00 ± 0.02 °C to mimic *in-vivo* conditions. The thermocouples functionalized with nanoMIPs are inserted into the liquid inside the flow cell 1.7 mm above the sensor surface of the chip. This temperature is defined as T_2 and measurements take place every second. In all measurements, the flow cells were filled with a solution of PBS and were left for 45 min to ensure stabilization of the baseline temperature signal measured by the functionalized thermocouple. Solutions (3 mL) of the target biomarker (H-FABP 1.5 – 75 ng/mL; ST2 3.15 – 315 ng/mL) were prepared in PBS or in FBS (ST2 63 – 1575 ng/mL) prior to experiments and stored at 4 °C until required. Each biomarker injection was performed at 250 µL/min for 12 min using an automated NE500 programmable syringe pump (ProSense, Oosterhout, the Netherlands). Following each sample addition, the system was allowed to stabilize for 30 min prior to the next injection. The thermal resistance (R_{th}) was determined throughout the whole measurement by dividing the temperature gradient ($T_1 - T_2$) over the power required to keep the heat sink at the set

temperature.[22] The R_{th} alongside the standard deviation of each thermocouple was calculated using the average of 600 data points before the beginning of each injection. This data was used to construct standard dose-response curves, from which the Limits of Detection (LoD) were calculated using the three sigma method in the linear range of the sensor. To establish the selectivity of the sensor in the single flow cells, measurements were performed with additions of another protein (BSA). In both the dual and triple cell systems an un-functionalized thermocouple was placed in the cell alongside the functionalized thermocouple to act as a control. To determine the selectivity in the triple thermocouple set-up, a thermocouple functionalized with the alternative biomarker nanoMIPs was used.

Modelling of Heat Flow through Flow Cell Designs Computational fluid dynamic (CFD) modelling was undertaken using Ansys Fluent V18.1 to give additional insight into the flow of heat within the cells. This was performed for both the single and triple thermocouple designs. Transient simulations were performed using a time-step of 0.5 s, which was selected following a time-step independence study. Mesh densities were optimized *via* a grid independence study: 174,077 cells for the single thermocouple design, 380,946 cells for the triple thermocouple design. Approximately double the number of cells were required for the triple thermocouple design primarily due to the need for finer meshing in the regions of close proximity. The boundary conditions were defined as follows: 1) Heat source, bottom surface of fluid domain was defined as a copper block with a constant temperature of 37 °C located 5 mm from the fluid domain. 2) Heat sink, top surface of fluid domain was defined as the heat lost through a 1.3 mm poly-L-lactic acid (PLLA) wall *via* convection to the environment at a bulk air temperature of 20 °C, with a film heat transfer coefficient of 25 $Wm^{-2}K^{-1}$. 3) All other surfaces were defined as adiabatic. Standard settings for modelling free convection in Fluent were used, as outlined in the Fluent V18.1 user guide. This included the use of the Boussinesq approximation, which was suitable in this case due to the small temperature differences in the flow cell (initial fluid temperature of 20 °C, surroundings of 20 °C and heat source of 37 °C). The fluid was modelled as pure water. Each simulation was run for a total of 600 time steps, giving 300 s of simulation data per case, and each achieved an approximate steady state as indicated by the levelling off of temperature and velocity fields. Solving each model took approximately 3 h, performed on a Dell OptiPlex 7060, with an Intel i5-8500 CPU (6 cores) and 16 gb of RAM. Velocity and temperature fields were exported from the simulation for post processing in the Ansys CFD-POST application.

Results and Discussion: Production and Charactization of nanoMIPs The synthesized nanoMIPs were characterized based on their size and affinity for their target biomarkers. The hydrodynamic diameter of the synthesized nanoMIPs at 25 °C in distilled water was 280 ± 18 nm for the ST2 nanoMIPs and 195 ± 4 nm for the H-FABP nanoMIPs. SPR analysis (Supporting Information S-3) revealed that a K_d value of 14 nM was obtained for the ST2 nanoMIPs whereas for the H-FABP nanoMIPs the K_d was estimated at 4 nM.

Thermal Experiments with nanoMIPs Functionalized Thermocouples Dip-coating was used to functionalize nanoMIPs for ST2 and H-FABP onto the thermocouples. Subsequently, these functionalized thermocouples were inserted into a single flow cell (Supporting Information S-2 A) which has been previously reported in literature and can measure one thermocouple at a time. The thermocouples were exposed to PBS solutions with increasing concentrations of the target molecule. In all cases, the temperature of the heat sink (T_1) was strictly controlled to 37.00 ± 0.02 °C whereas T_2 was solely monitored. Previous research has demonstrated that binding of the target to the imprints in the nanoMIPs increases the resistance at the solid-liquid interface, which leads to lower temperatures of T_2 being recorded by the thermocouple and thus higher R_{th} values.[22] Results depicting the measured temperature over time for the ST2 functionalized thermocouple and H-FABP functionalized thermocouple are presented in Supporting Information (S-4 B and C respectively). These figures clearly demonstrate a decrease in the temperature upon increasing the concentration of the appropriate biomarker due to binding of the protein to the polymer recognition layer. A similar response was observed for both cardiac biomarkers; whereas, upon the addition of a different protein (BSA, Supporting Information S-5 B and C) there was no significant change in the in the measured R_{th} values. This provided evidence toward the specificity of the nanoMIPs recognition elements. After providing proof-of-principle, other flow cell designs were explored in order to facilitate multiplexing and to minimize the influence of external parameters. An initial experiment consisted of connecting two single flow cells together in series and comparing the response of an ST2 functionalized thermocouple to that of a blank (non-functionalized) thermocouple (Supporting Information S-6). These results demonstrated decreases in T_2, corresponding to the functionalized thermocouple, whereas the temperature of the blank thermocouple remained unaffected. The main drawback of putting two flow cells in series is the requirement for double the sample size, which is not feasible in a clinical setting. Therefore, the initial design was adapted and novel flow cells were 3D printed. In the first set of flow cells, one additional inlet was added directly opposite the initial thermocouple inlet. This allowed for the simultaneous measurement of two thermocouples in the same flow cell. Figure 1 shows the raw data plots of R_{th} over time for additions of ST2 to a flow cell containing an ST2 functionalized thermocouple and an un-functionalized thermocouple (figure 1B). In PBS, the R_{th} value stabilized at 3.69 ± 0.04 °C/W for the blank thermocouple and 4.36 ± 0.05 °C/W for the functionalized thermocouple. These differences in stabilized R_{th} values can be affected by different variables including increased resistance due to the presence of particles on the thermocouple surface. Significant changes in the R_{th}, with respect to the baseline stabilization, were determined with concentrations of 6.3 ng/mL and higher, with a dynamic range of the sensor between 6.3 ng/mL and 63 ng/mL. Upon the addition of 6.3 ng/mL an increase in the absolute R_{th} was observed on the functionalized thermocouple from its baseline of 4.36 ± 0.05 °C/W to 4.49 ± 0.05 °C/W. This corresponded to a 3.0 ± 1.6 % increase in the R_{th} signal. The increase in the R_{th} continued for the additions of ST2 up until the final addition of 315 ng/mL where the R_{th} had increased to 4.75 ± 0.05 °C/W, corresponding in an 8.9 ± 1.6 % increase from the baseline level. These results were plotted in the form of a dose-response curve (figure 1 D, red circles), which was used to calculate a limit of detection (LoD) of 20 ± 4 ng/mL which corresponded to 312 ± 66 pM. Therefore, in addition to the simultaneous measurement of a blank thermocouple to improve reliability, this system showed a ten-fold increase in the sensitivity compared to the 5 nM LoD obtained

in previous work on protein detection using nanoMIPs.[22] In further experiments, it was studied whether this technique could be extended to the biomarker H-FABP.

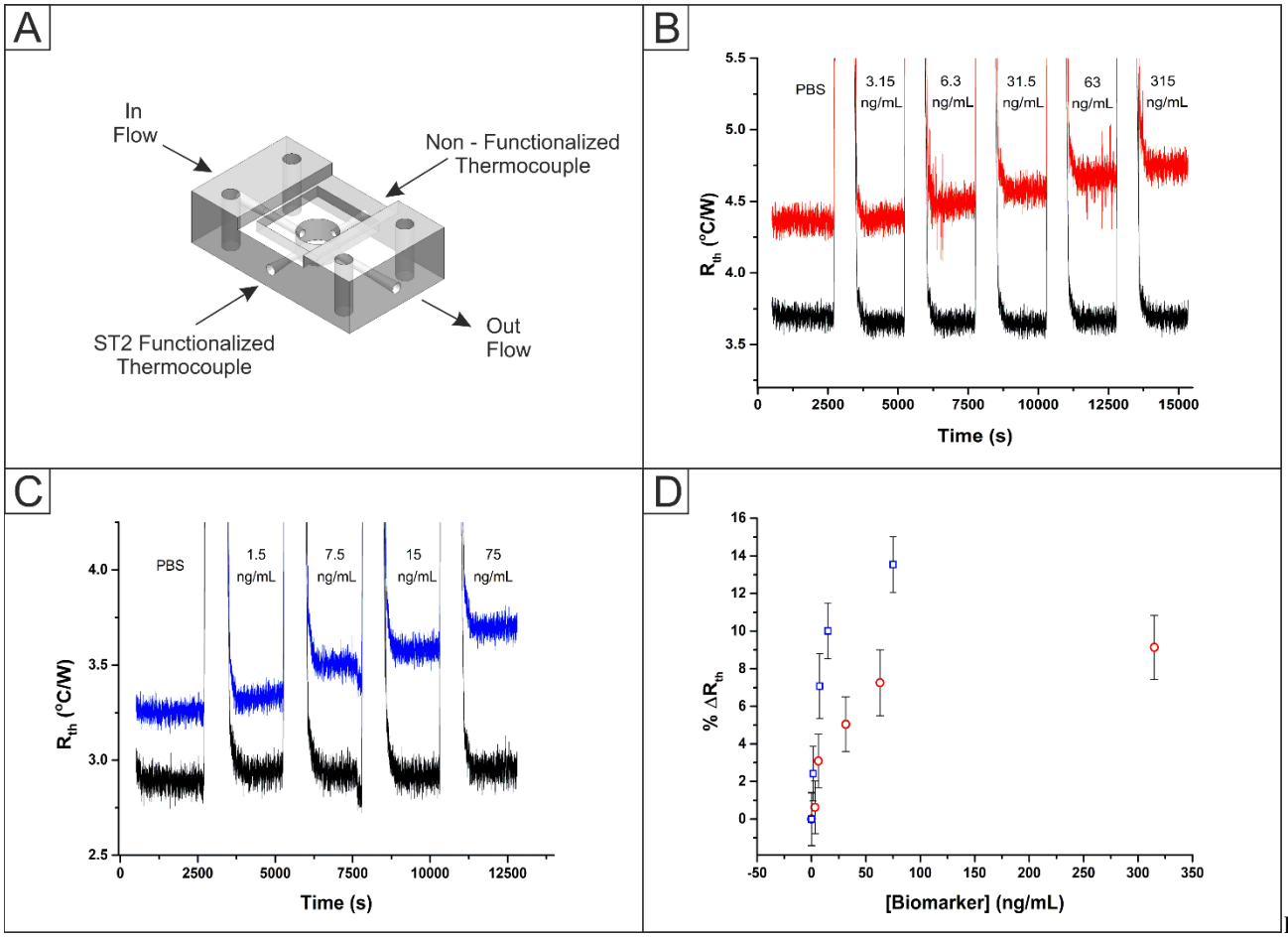

Figure 1. A) Schematic of the dual thermocouple flow cell used. B) Raw data HTM plot of the R_{th} over time for the addition of ST2 (3.15 – 315 ng/mL) in PBS to a dual thermocouple set-up with one thermocouple functionalized with ST2 nanoMIPs (red) and one un-functionalized thermocouple (black). C) Raw data HTM plot of the R_{th} over time for the addition of H-FABP (1.5 – 75 ng/mL) in PBS to a dual thermocouple set-up with one thermocouple functionalized with H-FABP nanoMIPs (blue) and one un-functionalized thermocouple (black). D) Dose-response curve for the addition of ST2 (3.15 – 315 ng/mL) in PBS to an ST2 nanoMIP functionalized thermocouple (red circles) and H-FABP (1.5 – 75 ng/mL) in PBS to an H-FABP nanoMIP functionalized thermocouple (blue squares) in the dual thermocouple set-up.

Figure 1C exhibits the raw data R_{th} response for a dual thermocouple flow cell in which one thermocouple is functionalized with H-FABP nanoMIPs (blue) and the other thermocouple is un-functionalized. This once again clearly demonstrated an increase in the measured R_{th} for the functionalized thermocouple upon the addition of target biomarker. In PBS, the R_{th} values stabilized at 2.88 ± 0.04 °C/W for the un-functionalized thermocouple and at 3.26 ± 0.03 °C/W for the H-FABP functionalized thermocouple. Significant changes in the measured R_{th} for the H-FABP functionalized thermocouple were observed upon the addition of 1.5 ng/mL with a working range up to 75 ng/mL. Upon the addition of 1.5 ng/mL of H-FABP, the R_{th} measured at the functionalized thermocouple increased to 3.34 ± 0.03 °C/W, corresponding to an increase of 2.5 ± 1 .3% from the baseline value. The increase in R_{th} continued up to the last injection of 75 ng/mL where it reached 3.70 ± 0.04 °C/W, corresponding to an increase of 13.5 ± 1.5 %. Once again this allowed for the conversion into a dose-response curve and elucidation of a LoD of 4.18 ± 0.73 ng/mL.

To improve the performance of the sensing platform the flow cell design was further modified to incorporate an additional thermocouple. This was done by elongating the inner chamber of the flow cell (Supporting Information S-2D), which increased the cell volume by 20 µL. The extension of the inner chamber permitted the staggering of thermocouple insertion points and allowed for the now parallel thermocouples to span the entire width of the flow cell chamber; meaning it is possible to control the insertion depth of each thermocouple. The addition of an extra thermocouple allowed for another control to be added to the system; by functionalizing one thermocouple with nanoMIPs for the biomarker not being used as a target. The results of this experiment, where the first thermocou-

ple was functionalized with H-FABP, the second with the target nanoMIPs ST2 and the third thermocouple was left un-functionalized are presented in Figure 2.

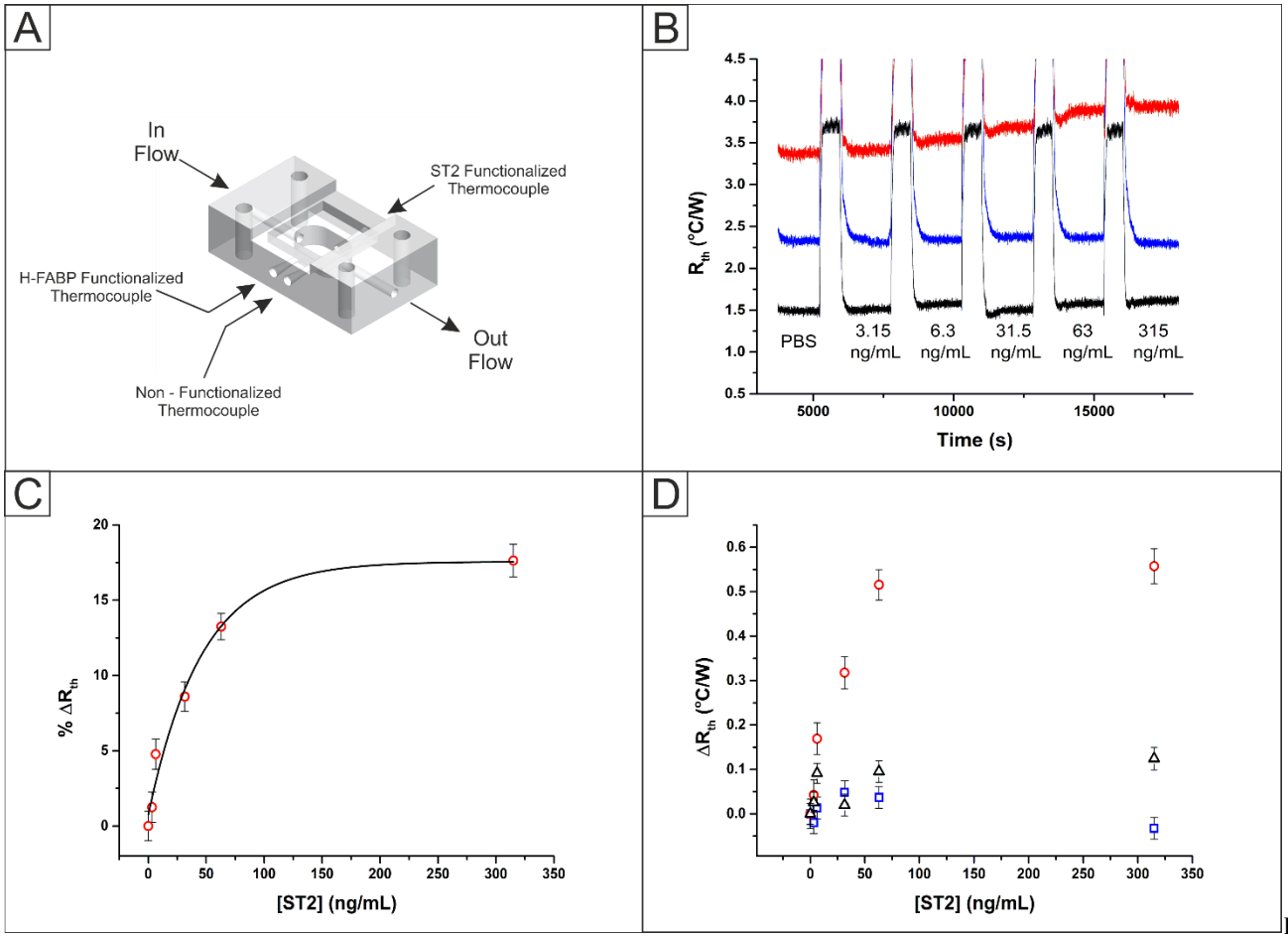

Figure 2. A) Schematic of the triple thermocouple flow cell used. B) Raw data HTM plot of the R_{th} over time for the addition of ST2 (3.15 – 315 ng/mL) in PBS to a triple thermocouple set-up with one thermocouple functionalized with ST2 nanoMIPs (red), one functionalized with H-FABP nanoMIPs (blue) and one un-functionalized thermocouple (black). C) Dose-response curve for the addition of ST2 (3.15 – 315 ng/mL) in PBS to a thermocouple functionalized with ST2 nanoMIPs in a triple thermocouple set-up. D) Plot showing the change in R_{th} value *versus* the concentration of ST2 injected into the flow cell for each thermocouple (red circles = ST2, blue square = H-FABP and green triangles = Blank.

In PBS, the R_{th} values stabilized at 3.38 ± 0.03 °C/W for the ST2 nanoMIP functionalized thermocouple, 2.33 ± 0.02 °C/W for the H-FABP nanoMIP functionalized thermocouple and 1.49 ± 0.02 °C/W for the un-functionalized thermocouple. The functionalized thermocouples were expected to have a larger baseline stabilization R_{th} value then the un-functionalized thermocouple due to the presence of the insulating plastic nanoparticles on their surface. However, the major reason for variations in thermocouple stabilization values is the variance in manufacturing. This variance is shown in Supporting Information S-7B. Although the absolute temperature values measured were shown to vary by up to 1.5 °C, once the stabilization value was reached the accuracy of this measurement was maintained with a standard deviation of ± 0.01 °C calculated over 600 data points. The position of the thermocouple inside the flow cells, meaning whether the thermocouple is in the front, middle or back of the cell, has minimal effect on the measurement as seen in Supporting Information S-7C. This showed only small variations in measured temperature when the thermocouples were shifted to a different position and a temperature gradient applied.

Upon the addition of 6.3 ng/mL of ST2, the R_{th} value measured at the ST2 nanoMIP functionalized thermocouple increased to 3.54 ± 0.04 °C/W, corresponding to an increase of 4.7 ± 1.5 % from the baseline value. This increase in the R_{th} continued up until the last injection of 315 ng/mL where the R_{th} reached 3.93 ± 0.04 °C/W, corresponding to an increase of 16.3 ± 1.5 %. The percentage increase observed for the triple cell system was almost double that observed in the double cell for the same concentration range of ST2. The raw data was converted into a dose-response curve, figure 3C, which allowed the elucidation of an LoD of 8.79 ± 0.79 ng/mL or 140 ± 13 pM. Therefore, the LoD had exhibited a decrease of over 50 %. The improvements observed when switching from the single/double cell design

to the triple cell were explained through computational modelling (Supporting Information S7). The triple cell reaches a steady temperature faster than the single cell. In this configuration it was seen that the central thermocouple is consistently 0.6 °C lower than the other two thermocouples. The average velocity magnitude was observed to be lower in the triple cell which is seen in the reduced noise values. This is explained by the smaller aspect ratio (height/hydraulic diameter) in the three thermocouple system; where this suppressed the natural convection leading to a lower velocity magnitude and more stable signal. A comparison of the LoD's achieved in literature and this work are presented in Table 1. The other sensing methodologies reported showed LoD's an order of magnitude lower than this report; however, this work presented key advantages such as the multiplexing, greatly reduced costs and ease of sensor preparation whilst still providing analyte detection in the clinically relevant concentration ranges. The dip-coating method, although simple, can be improved substantially in the future which would be expected to further enhance sensor performance.

Table 1. Comparison table for the published methods of detection for H-FABP and ST2 biomarkers.

Biomarker	Recognition Element	Read-Out Method	Format	LoD (ng/mL)	Ref.
H-FABP[a]	AB's[b]	Capacitive	Single	0.836	[25]
H-FABP[a]	AB's[b]/QD's[c]	Fluorescence	Single	0.221	[26]
H-FABP[a]	AB's[b]	ELISA[d]	Single	0.3	[27]
ST2	AB's[b]	ELISA[d]	Single	1.3	[28]
H-FABP[a]	nanoMIPs	Thermal	Multiplex	4.18	This Work
ST2	nanoMIPs	Thermal	Multiplex	8.79	This Work

[a]Heart Fatty Acid Binding Protein, [b]Antibodies, [c]Quantum Dots, [d]Enzyme-Linked Immunosorbent Assay.

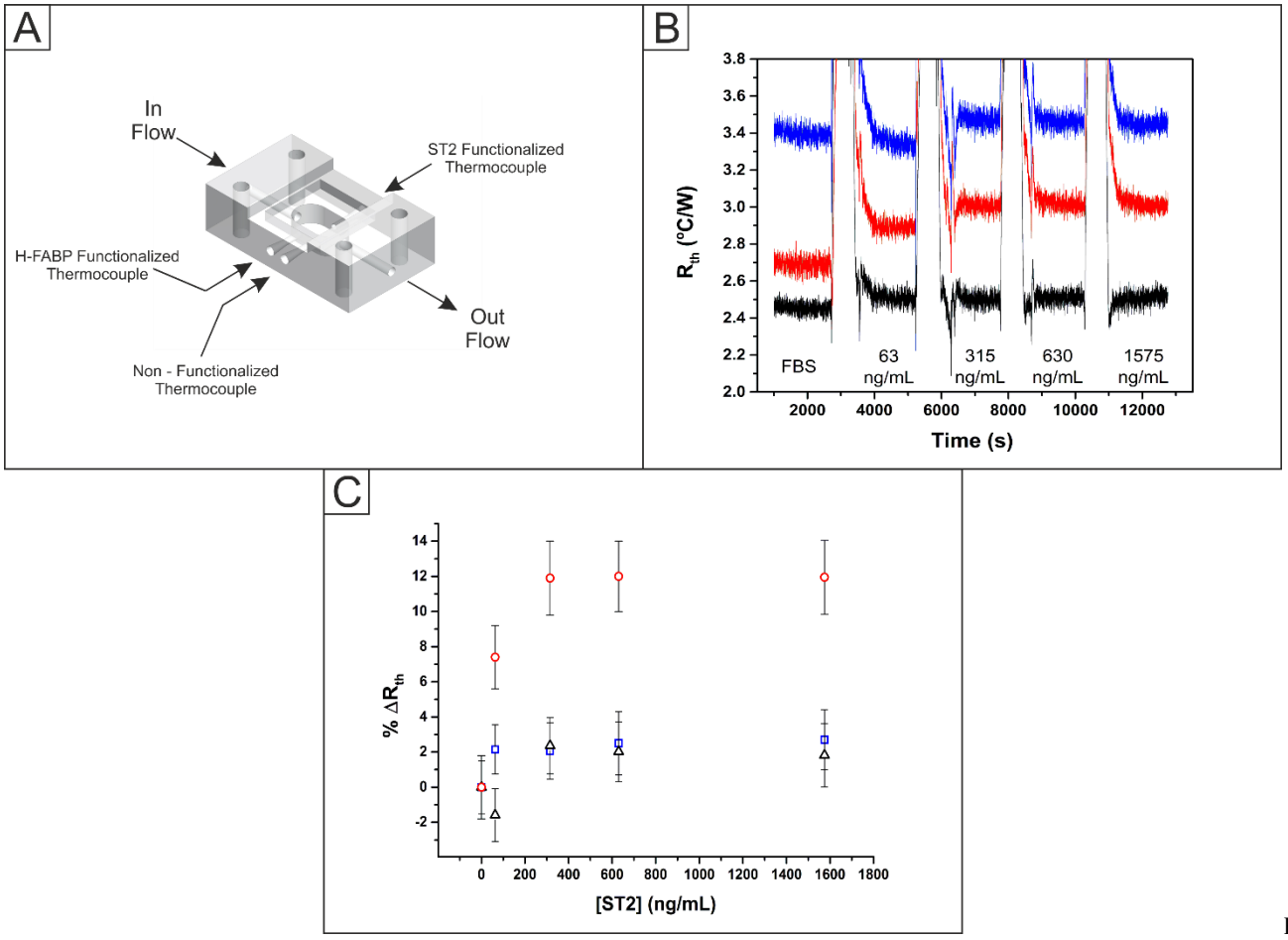

Figure 3. A) Schematic of the triple thermocouple flow cell used. B) Raw data HTM plot of the R_{th} over time for the addition of ST2 (63 – 1575 ng/mL) in FBS to a triple thermocouple set-up with one thermocouple functionalized with ST2 nanoMIPs (red), one functionalized with H-FABP nanoMIPs (blue) and one un-functionalized thermocouple (black). C) Plot of the R_{th} % change for the addition of ST2 (63 – 1575 ng/mL) in FBS to a triple thermocouple set-up with one thermocouple functionalized with ST2

nanoMIPs (red circles), one functionalized with H-FABP nanoMIPs (blue squares) and one un-functionalized thermocouple (green triangles).

To provide a proof-of-application, an experiment was performed injecting fetal bovine serum (FBS) that was spiked with ST2 (63 ng/mL – 1575 ng/mL), Figure 3. In FBS, the R_{th} stabilized at 2.69 ± 0.04 °C/W for the ST2 nanoMIP functionalized thermocouple, 3.39 ± 0.04 °C/W for the H-FABP functionalized thermocouple and 2.45 ± 0.03 °C/W for the un-functionalized thermocouple. There was an observed increase in the noise on the raw data signals and the system takes noticeably longer to reach stabilization due to the more complex nature of the matrix. This included non-specific binding of proteins to the thermocouples and nanoMIPs. Upon the addition of 63 ng/mL ST2 there is a larger increase in the measured R_{th} for the ST2 functionalized thermocouple to 2.89 ± 0.03 °C/W, corresponding to a 7.4 ± 1.8 % increase in the signal. This value is approximately 50 % lower than the increase of 1± 1.5 % observed in the PBS medium. The R_{th} measured at the ST2 nanoMIP functionalized thermocouple increased to a maximum for the addition of 315 ng/mL at a value of 3.01 ± 0.04 °C/W which corresponded to an increase of 11.9 ± 2.1 %. The increase in R_{th} measured at the ST2 nanoMIP functionalized thermocouple was five times greater than at either of the other thermocouples present, Figure 3C, showing the sensing platform had good selectivity for the target biomarker in FBS. This demonstrates the possibility for this type of sensing platform to act as a traffic light system for a death prediction cut-off points as reported by Pascual-Figal *et al.* [29]

Conclusions: MIP nanoparticles (size ranging from ~200-280 nm) for ST2 and H-FABP as target molecules were prepared according to a solid phase approach. This is the first report of nanoMIPs for these cardiac biomarkers in literature, with determined K_d values (4-14 nM) comparable to that of commercially available antibodies. Thermocouples were functionalized with nanoMIPs *via* dip coating and inserted into flow cells that were coupled to a home-made thermal measurement device. Addition of buffered solutions containing the relevant cardiac biomarkers resulted in an increase of the thermal resistance at the solid-liquid interface of the functionalised thermocouple. This resulted in a lower temperature recorded in the fluid. Dose-response curves were constructed to correlate the biomarker concentration to the thermal resistance. Different flow cell designs were explored, with computational modelling providing insight into the optimal configuration by determining the heat distribution through the system. The developed sensor platform was capable to simultaneously measure ST2 and H-FABP, with minimal cross selectivity between the two markers. It was possible to measure both in buffered solutions and spiked serum solutions within the psychologically relevant range, demonstrating proof-of-application of the technology. The use of nanoMIPs combined with thermal read-out enables a multimarker strategy which could have high potential for sustainable healthcare due to its low-cost, straightforward operation, and ability to tailor the sensor towards the required target.

Supporting Information

Supporting Information available: The following files are available free of charge. nanoMIPscardiacbiomarkerdetection_20092019_SupportingInformation. The Supporting Information contains the details of the functionalisation procedure, SEM of a functionalised thermocouple, schematic of the flow cells used, SPR analysis of the nanoMIPs, and HTM measurements done on a single cell flow cell design. Further information on the cell set ups, the influence of the position of the thermocouple and computational modelling of the flow and heat-transfer within the cells is also provided.

AUTHOR INFORMATION

Corresponding Author

* Dr. Marloes Peeters (Marloes.Peeters@newcastle.ac.uk)

Author Contributions All authors have given approval to the final version of the manuscript.

Funding Sources

MP would like to acknowledge the EPSRC for funding under grant number EP/R029296/1 and NC3Rs for a CRACK IT grant to cover salary of RC.

ACKNOWLEDGMENT

MP would like to acknowledge the EPSRC for funding under grant number EP/R029296/1 and NC3Rs for a CRACK IT grant to cover salary of RC.

REFERENCES

1.Reaney, P. D.; Elliott, H. I.; Noman, A.; Cooper, J. G., Risk stratifying chest pain patients in the emergency department using HEART, GRACE and TIMI scores, with a single contemporary troponin result, to predict major adverse cardiac events. *Emerg Med J* **2018,** *35* (7), 420-427.

2.(a) Chacko, S.; Haseeb, S.; Glover, B. M.; Wallbridge, D.; Harper, A., The role of biomarkers in the diagnosis and risk stratification of acute coronary syndrome. *Future science OA* **2017,** *4* (1), FSO251; (b) Christenson, E.; Christenson, R. H., The role of cardiac biomarkers in the diagnosis and management of patients presenting with suspected acute coronary syndrome. *Annals of laboratory medicine* **2013,** *33* (5), 309-318.

3.Al-Hadi, H. A.; Fox, K. A., Cardiac markers in the early diagnosis and management of patients with acute coronary syndrome. *Sultan Qaboos University Medical Journal* **2009,** *9* (3), 231.

4.Cervellin, G.; Rastelli, G., The clinics of acute coronary syndrome. *Annals of translational medicine* **2016,** *4* (10).

5.Pickering, J. W.; Greenslade, J. H.; Cullen, L.; Flaws, D.; Parsonage, W.; Aldous, S.; George, P.; Worster, A.; Kavsak, P. A.; Than, M. P., Assessment of the European Society of Cardiology 0-hour/1-hour algorithm to rule-out and rule-in acute myocardial infarction. *Circulation* **2016,** *134* (20), 1532-1541.

6.Body, R.; Carley, S.; McDowell, G.; Pemberton, P.; Burrows, G.; Cook, G.; Lewis, P. S.; Smith, A.; Mackway-Jones, K., The Manchester Acute Coronary Syndromes (MACS) decision rule for suspected cardiac chest pain: derivation and external validation. *Heart* **2014,** *100* (18), 1462-1468.
7.Body, R.; Carlton, E.; Sperrin, M.; Lewis, P. S.; Burrows, G.; Carley, S.; McDowell, G.; Buchan, I.; Greaves, K.; Mackway-Jones, K., Troponin-only Manchester Acute Coronary Syndromes (T-MACS) decision aid: single biomarker re-derivation and external validation in three cohorts. *Emerg Med J* **2017,** *34* (6), 349-356.
8.Van Den Berg, P.; Body, R., The HEART score for early rule out of acute coronary syndromes in the emergency department: a systematic review and meta-analysis. *European Heart Journal: Acute Cardiovascular Care* **2018,** *7* (2), 111-119.
9.(a) Glatz, J.; Kleine, A.; van Nieuwenhoven, F. A.; Hermens, W. T.; van Dieijen-Visser, M.; Van der Vusse, G., Fatty-acid-binding protein as a plasma marker for the estimation of myocardial infarct size in humans. *Heart* **1994,** *71* (2), 135-140; (b) Tanaka, T.; Hirota, Y.; Sohmiya, K.-I.; Nishimura, S.; Kawamura, K., Serum and urinary human heart fatty acid-binding protein in acute myocardial infarction. *Clinical biochemistry* **1991,** *24* (2), 195-201.
10.(a) Banu, S.; Tanveer, S.; Manjunath, C., Comparative study of high sensitivity troponin T and heart-type fatty acid-binding protein in STEMI patients. *Saudi journal of biological sciences* **2015,** *22* (1), 56-61; (b) Willemsen, R. T.; van Severen, E.; Vandervoort, P. M.; Grieten, L.; Buntinx, F.; Glatz, J. F.; Dinant, G. J., Heart-type fatty acid binding protein (H-FABP) in patients in an emergency department setting, suspected of acute coronary syndrome: optimal cut-off point, diagnostic value and future opportunities in primary care. *European Journal of General Practice* **2015,** *21* (3), 156-163.
11.Hoffmann, U.; Espeter, F.; Weiß, C.; Ahmad-Nejad, P.; Lang, S.; Brueckmann, M.; Akin, I.; Neumaier, M.; Borggrefe, M.; Behnes, M., Ischemic biomarker heart-type fatty acid binding protein (hFABP) in acute heart failure-diagnostic and prognostic insights compared to NT-proBNP and troponin I. *BMC cardiovascular disorders* **2015,** *15* (1), 50.
12.McCann, C. J.; Glover, B. M.; Menown, I. B.; Moore, M. J.; McEneny, J.; Owens, C. G.; Smith, B.; Sharpe, P. C.; Young, I. S.; Adgey, J. A., Novel biomarkers in early diagnosis of acute myocardial infarction compared with cardiac troponin T. *European heart journal* **2008,** *29* (23), 2843-2850.
13.Coglianese, E. E.; Larson, M. G.; Vasan, R. S.; Ho, J. E.; Ghorbani, A.; McCabe, E. L.; Cheng, S.; Fradley, M. G.; Kretschman, D.; Gao, W., Distribution and clinical correlates of the interleukin receptor family member soluble ST2 in the Framingham Heart Study. *Clinical chemistry* **2012,** *58* (12), 1673-1681.
14.Konukoglu, D., Invited Review Is soluble ST2 a new marker in heart failure? *Int J Med Biochem* **2018,** *1* (1), 44-51.
15.Bayes-Genis, A.; Pascual-Figal, D.; Januzzi, J. L.; Maisel, A.; Casas, T.; Valdés, M.; Ordóñez-Llanos, J., Soluble ST2 monitoring provides additional risk stratification for outpatients with decompensated heart failure. *Revista Española de Cardiología (English Edition)* **2010,** *63* (10), 1171-1178.
16.Ho, J. E.; Sritara, P.; deFilippi, C. R.; Wang, T. J., Soluble ST2 testing in the general population. *The American journal of cardiology* **2015,** *115* (7), 22B-25B.
17.(a) Haupt, K.; Mosbach, K., Molecularly imprinted polymers and their use in biomimetic sensors. *Chemical reviews* **2000,** *100* (7), 2495-2504; (b) Takeuchi, T.; Haginaka, J., Separation and sensing based on molecular recognition using molecularly imprinted polymers. *Journal of Chromatography B: Biomedical Sciences and Applications* **1999,** *728* (1), 1-20.
18.Sellergren, B.; Allender, C. J., Molecularly imprinted polymers: A bridge to advanced drug delivery. *Advanced drug delivery reviews* **2005,** *57* (12), 1733-1741.
19.Poma, A.; Guerreiro, A.; Whitcombe, M. J.; Piletska, E. V.; Turner, A. P.; Piletsky, S. A., Solid-phase synthesis of molecularly imprinted polymer nanoparticles with a reusable template–"plastic antibodies". *Advanced functional materials* **2013,** *23* (22), 2821-2827.
20.(a) Canfarotta, F.; Poma, A.; Guerreiro, A.; Piletsky, S., Solid-phase synthesis of molecularly imprinted nanoparticles. *Nature protocols* **2016,** *11* (3), 443; (b) Cecchini, A.; Raffa, V.; Canfarotta, F.; Signore, G.; Piletsky, S.; MacDonald, M. P.; Cuschieri, A., In vivo recognition of human vascular endothelial growth factor by molecularly imprinted polymers. *Nano letters* **2017,** *17* (4), 2307-2312.
21.(a) Pan, J.; Chen, W.; Ma, Y.; Pan, G., Molecularly imprinted polymers as receptor mimics for selective cell recognition. *Chemical Society Reviews* **2018,** *47* (15), 5574-5587; (b) Spivak, D. A., Optimization, evaluation, and characterization of molecularly imprinted polymers. *Advanced drug delivery reviews* **2005,** *57* (12), 1779-1794.
22.Canfarotta, F.; Czulak, J.; Betlem, K.; Sachdeva, A.; Eersels, K.; Van Grinsven, B.; Cleij, T.; Peeters, M., A novel thermal detection method based on molecularly imprinted nanoparticles as recognition elements. *Nanoscale* **2018,** *10* (4), 2081-2089.
23.Van Grinsven, B.; Eersels, K.; Peeters, M.; Losada-Pérez, P.; Vandenryt, T.; Cleij, T. J.; Wagner, P., The heat-transfer method: a versatile low-cost, label-free, fast, and user-friendly readout platform for biosensor applications. *ACS applied materials & interfaces* **2014,** *6* (16), 13309-13318.
24.Geerets, B.; Peeters, M.; Grinsven, B.; Bers, K.; De Ceuninck, W.; Wagner, P., Optimizing the thermal read-out technique for MIP-based biomimetic sensors: Towards nanomolar detection limits. *Sensors* **2013,** *13* (7), 9148-9159.
25.Mihailescu, C.-M.; Stan, D.; Iosub, R.; Moldovan, C.; Savin, M., A sensitive capacitive immunosensor for direct detection of human heart fatty acid-binding protein (h-fabp). *Talanta* **2015,** *132*, 37-43.
26.Savin, M.; Mihailescu, C.-M.; Matei, I.; Stan, D.; Moldovan, C. A.; Ion, M.; Baciu, I., A quantum dot-based lateral flow immunoassay for the sensitive detection of human heart fatty acid binding protein (hFABP) in human serum. *Talanta* **2018,** *178*, 910-915.
27.Wodzig, K. W. H.; Pelsers, M. M.; van der Vusse, G. J.; Roos, W.; Glatz, J. F., One-step enzyme-linked immunosorbent assay (ELISA) for plasma fatty acid-binding protein. *Annals of clinical biochemistry* **1997,** *34* (3), 263-268.
28.Dieplinger, B.; Mueller, T., Soluble ST2 in heart failure. *Clinica Chimica Acta* **2015,** *443*, 57-70.
29.Pascual-Figal, D. A.; Manzano-Fernández, S.; Boronat, M.; Casas, T.; Garrido, I. P.; Bonaque, J. C.; Pastor-Perez, F.; Valdés, M.; Januzzi, J. L., Soluble ST2, high-sensitivity troponin T-and N-terminal pro-B-type natriuretic peptide: complementary role for risk stratification in acutely decompensated heart failure. *European journal of heart failure* **2011,** *13* (7), 718-725.

For TOC Only

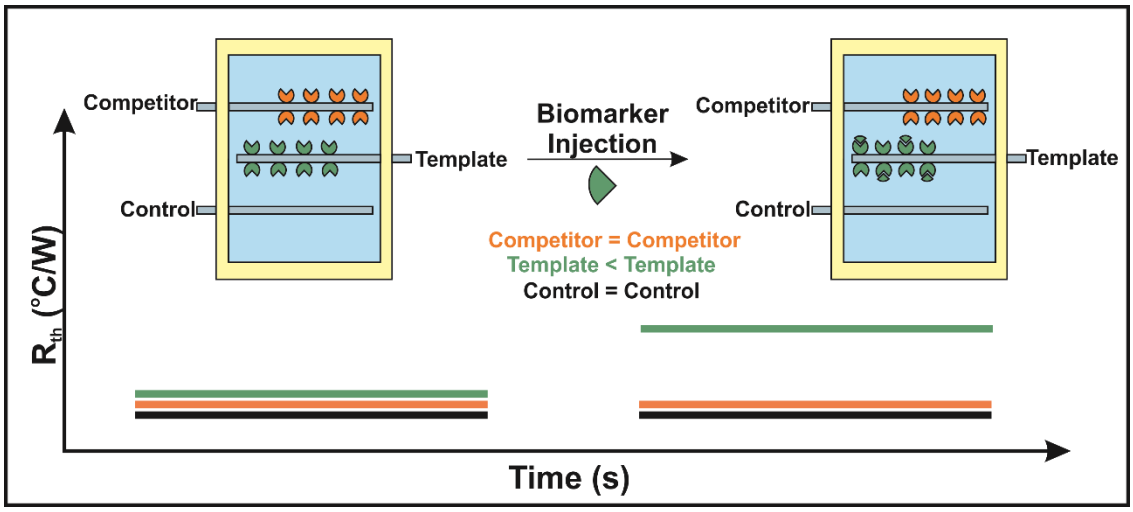
Competitor
Control
Template
Biomarker Injection
Competitor
Control
Template
Competitor = Competitor
Template < Template
Control = Control
R_{th} (°C/W)
Time (s)